
CCFL: Computationally Customized Federated Learning

Hao Zhang

Department of Computer Science
Harbin Institute of Technology
Harbin, China 150000
zh1000@hit.edu.cn

Tingting Wu

Department of Computer Science
Harbin Institute of Technology
Harbin, China 150000
ttwu@ir.hit.edu.cn

Siyao Cheng

Department of Computer Science
Harbin Institute of Technology
Harbin, China 150000
csy@hit.edu.cn

Jie Liu

the Institute for Artificial Intelligence
Harbin Institute of Technology (Shenzhen)
Shenzhen 518055, China
jieliu@hit.edu.cn

Abstract

Federated learning (FL) is a method to train model with distributed data from numerous participants such as IoT devices. It inherently assumes a uniform capacity among participants. However, participants have diverse computational resources in practice due to different conditions such as different energy budgets or executing parallel unrelated tasks. It is necessary to reduce the computation overhead for participants with inefficient computational resources, otherwise they would be unable to finish the full training process. To address the computation heterogeneity, in this paper we propose a strategy for estimating local models without computationally intensive iterations. Based on it, we propose Computationally Customized Federated Learning (CCFL), which allows each participant to determine whether to perform conventional local training or model estimation in each round based on its current computational resources. Both theoretical analysis and exhaustive experiments indicate that CCFL has the same convergence rate as FedAvg without resource constraints. Furthermore, CCFL can be view of a computation-efficient extension of FedAvg that retains model performance while considerably reducing computation overhead.

1 Introduction

With the rapid development of the Internet of Things (IoT), the number of IoT devices (e.g., smart phones, cameras and sensing devices) has increased dramatically. These devices are playing an increasingly important role in people's lives. They continually create large volumes of data, which encourages the use of artificial intelligence technology to improve a number of existing applications, including smart healthcare systems, automated driving, etc. However, due to the privacy concerns and communication limitations, keeping data locally is becoming increasingly appealing. Federated learning (FL) [1], which allows devices to collectively train a model without sharing local data, is emerging to make use of this dispersed data across a range of devices.

Normally, a stable global model of FL is achieved after multiple rounds of local training and global aggregation. At each round, all or a portion of participants (usually selected by the server) calculate an updated model based on their local data, which is commonly iterated numerous times using optimization methods such as stochastic gradient descent (SGD) or its variations. This local

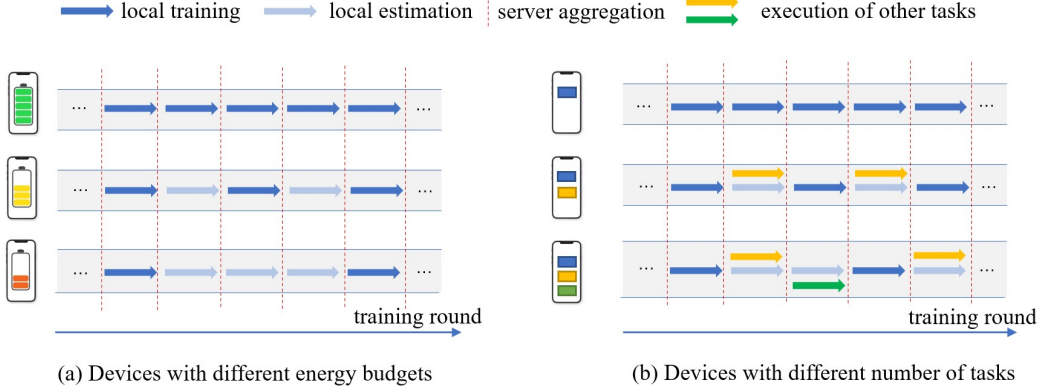


Figure 1: Illustration of CCFL solving computation heterogeneity in FL training. “Local training” refers to the traditional iterative method (e.g., SGD) to obtain local models, which is computationally expensive. “Local estimation” refers to estimating the local model from historical information with negligible computational overhead. (a) Devices schedule to train or estimate local models in advance based on their energy budgets. (2) Devices decide whether to execute local training or local estimation based on the tasks in time.

training requires intensive on-device computing for long periods. However, devices in the wild greatly vary in computational resource budgets, resulting in some devices’ computing resources being insufficient to enable training. Even for the identical devices, resource budgets may still vary dramatically and dynamically. For instance, the devices with low energy budgets cannot provide enough computation capability to complete the entire training. Or other unrelated tasks that consume an arbitrary percentage of the resource, prevent the devices from providing sufficient computational resources for training. This ubiquitous presence of *computation heterogeneity* is not considered by conventional FL methods, represented FedAvg. In fact, in both cross-silo and cross-device settings [2], all the clients have the same computational cost for conventional FL methods both in theoretical analysis and practical applications [3, 4]. Devices with insufficient computational capacity cause straggler issues [1, 5] (e.g., the devices are busy during training) or even drop-out issues [6, 7] (e.g., the battery is consumed during training), which slows down training and harms performance [8].

To complete the entire training process, devices would reduce the number of participating training rounds. They skip certain training rounds even when they are required to participate (e.g., selected by the server) in order to conserve limited computational resource. In this way, the server would not receive the expected local models from these devices in the corresponding rounds. There are two intuitive strategies to deal with these devices. The first is to ignore them, aggregating global model only from the received local models (Strategy 1). This is how the original FedAvg [1] does. However, it introduces bias into training data [5], because the devices with sufficient computational resources participate more frequently, resulting in over-representation of their local data, and vice versa. Moreover, if numerous devices skip the training, there will be insufficient participants, making the model’s performance unstable [9]. The second is to utilize the latest local models of these devices [8] (Strategy 2), so that all devices participate in training with the same number of rounds. However, this strategy uses stale models, which decreases the performance of the global model. As a result, the devices lacking of computational resources are required to provide new local model in corresponding rounds while avoiding substantial computational cost. To meet this requirement, we try to “guess” the local model as close as possible to the model obtained by training locally. Actually, for each client the latest local model can be regarded as an estimated one in current round, but it has large difference from the trained model.

In this paper, we propose a strategy for estimating the local model without computationally intensive iterations. Specifically, we estimate the newly local model using historical information. We observe that the model estimation is much closer to the trained one than that estimated by Strategy 2, especially at the early stage of training. Based on this strategy, we propose Computationally Customized Federated Learning (CCFL), which can train FL models across clients with heterogeneous computational

resources. CCFL allows the selected clients to determine whether to perform local training based on their computational resources at each training round (illustrated in Fig. 1). The main contributions of this paper can be summarized as follows:

- We study the problem of computation heterogeneity in FL, and present a strategy for estimating the local model to be close to the model derived through local training while consuming very little computing computational resources (only need one vector addition).
- Inspired by the preceding strategy, we propose CCFL, which allows clients with diverse computational resources to train FL model collaboratively. We prove that CCFL has the same convergence speed as vanilla FedAvg without limitation of computational resources (FedAvg for short). Our evaluation demonstrate that the performance of CCFL is almost the same as FedAvg, and much better than other two FL baselines under heterogeneous budget constraints.
- Meanwhile, CCFL can be thought of a computation-efficient extension of FedAvg that can save computational resources many times while retaining performance. It can replace FedAvg in any scenarios without limiting to tackle computation heterogeneity. From the experiments CCFL retains the model performance even when the computation cost is reduced to $1/4$ for each participant.

2 Related Work

In practice the great variability of devices makes it challenging to deploy FL in the wild. Various kinds of heterogeneity need to be addressed.

Data heterogeneity. Data heterogeneity is the most attractive topic, which starts with the birth of FL [1]. It is assumed that data are distributed across participants in a non-IID way, which results in large gaps among local models, aggregating a global model with poor performance [10]. Pioneer works like [11, 12, 13] correct the client drift actively to reduce the gaps among local models. Others like [14, 15, 16, 17] introduce regularization to reduce the difference between local models.

Device heterogeneity. In contrast to the significant work spent to data heterogeneity, tackling device heterogeneity has received less attention. [18, 19, 20, 21] address on system heterogeneity (mainly on run-time memory heterogeneity where participants are with different on-chip memory budgets). These methods enables devices to train size-adjustable local models based on their memory budgets, eliminating the constraint of standard FL methods that the global model complexity is limited for the most indigent device. Smaller models require fewer computational resources to train, but at the expense of performance. Thus these methods are not suitable for the scenario of this paper.

At present computation heterogeneity is partly considered by some works. [22] handles the problem by selecting participants based on their resource information. However, a biased global model may be obtained because clients with more resources participate more. Some works such as [23, 24] utilize model distillation for FL, where the architecture of local models can be decided based on participants' resources, but these methods usually rely on public datasets for knowledge transmission, which may not be realistic. Energy consumption is strongly correlated with computation overhead. [25, 26] minimize the total energy cost in FL training, whilst ignoring device heterogeneity. [27] proposes an energy-aware FL selection method based on the uploaded participants' profiles to balance the energy consumption across these battery-constrained devices. [28] exploits reinforcement learning to choose participants in each training round. However, these methods are still biased selection, resulting in a model that differs from the deterministic aggregation of all clients [9].

Training efficiency. Numerous studies try to speed up the training of FedAvg. SCAFFOLD [11] achieves comparable performance to FedAvg by altering the local models. CMFL [29] analyzes local models before uploading to avoid upload irrelevant update. FedCos [17] introduces a cosine regularization term to reduce the directional inconsistency of local models. FedDyn [30] uses linear and quadratic penalty terms to make local minima and global stationary point consistent. However, all of these methods incur more storage and calculation cost than FedAvg. Instead, our approach improves training effectiveness with almost any additional expense on FedAvg.

3 Computationally Customized Federated Learning

3.1 Federated Learning and Computation Heterogeneity

We focus on federated training, in which N edge clients are collaborated to yield a global model under the coordination of a parameter server. Formally, the goal is to solve the optimization problem as

$$\min_{x \in \mathbb{R}^d} f(x) = \frac{1}{N} \sum_{i=1}^N f_i(x), \quad (1)$$

where $f_i(x) := \mathbb{E}_{\xi \sim \mathcal{D}_i}[\ell_i(x, \xi)]$ is the local loss of the i -th client with local dataset \mathcal{D}_i . For normal federated learning methods such as FedAvg, the training process is divided into T rounds. In the t -th round ($t < T$), the server randomly selects a part of clients (or all of them) denoted as \mathcal{S}_t and broadcasts the global model x_t , which is aggregated in the latest round (for $t = 0$, x_0 is randomly initialized by the server). Each client received x_t initializes its local model $x_{t,0}^i = x_t$, and then performs K SGD steps iteratively on local dataset with learning rate η as

$$x_{t,k+1}^i = x_{t,k}^i - \eta g_{t,k}^i, k = 0, 1, \dots, K-1, \quad (2)$$

where $g_{t,k}^i$ is an unbiased estimator in each step, i.e., $\mathbb{E}[g_{t,k}^i] = \nabla f_i(x_{t,k}^i)$.

After K steps of iteration, the server aggregates updated local models by

$$x_{t+1} = \frac{1}{|\mathcal{S}_t|} \sum_{i \in \mathcal{S}_t} x_{t,K}^i. \quad (3)$$

In the regular federated learning process, all clients consume the same amount of computational resources in expectation. In actuality, however, they do not have the same computational resource budgets. This is referred to as *computation heterogeneity*. For example, due to lack of in energy reserves, some clients are unable to execute the same amount of computation as others. Even in the absence of energy constraints, the imbalance of computing resources still exists. For instance, while performing federated training, the client may process multiple other tasks concurrently. Because of resource preemption, the computational resources for some participants in federated training are insufficient. As a result, these clients with insufficient computational resources are unable to complete K iterations before a predetermined time in one round. They would be regarded as “stragglers”, even drop out the training [7].

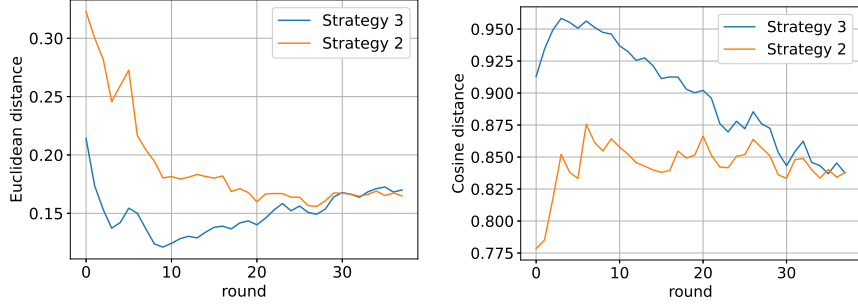
3.2 Motivation and Baselines

To address this issue, we should balance computing overhead among clients with heterogeneous computational resources, i.e., we should reduce the computation load of clients with inefficient computational resources to avoid bottlenecks. Formally, for client i in federated learning, the ratio of remaining computational overhead (compared with the overhead in traditional FL) is denoted as $p_i \in (0, 1]$. Since the computational resources of clients are mainly consumed in the iterations of gradient updates. The scarcer the computational resource of client is, the smaller p_i is. Particularly, if the client has sufficient resources, $p_i = 1$. The intuitive way to lower computational overhead is to reduce the number of local iteration. Specifically, for round t , if client i is in \mathcal{S}_t , it skips local iterations in this round with probability $1 - p_i$. In the whole training process, client i calculates gradients by $p_i \times K \times T$ times, while it needs $K \times T$ times in traditional FL. Hence the computation cost is reduced by $1 - p_i$ totally.

In aggregation phase, the server would deal with the clients skipping local training. Accordingly, there are two intuitive ways to deal with these clients. The first is to ignore them directly, forming the strategy as

Strategy 1 *If client i will skip the current training round, it sends back "skip" signal to the server (or the client is unavailable). The server removes it from \mathcal{S}_t in aggregation phase.*

This strategy is how original FedAvg addresses computation heterogeneity [1]. Strategy 1 ensures that the computing consumption meets the requirement of clients with heterogeneous computational resources, but it leads to a bias client sampling scheme, leading the aggregated model to be different



(a) Euclidean distance (the smaller the better) (b) Cosine distance (the larger the better)

Figure 2: We investigate the deviation between the estimated models and the true models by different strategies for one random chosen client (indexed by i). In (a) we measure the Euclidean distances between the estimated models and the true models. For Strategy 2, it is $\|x_{t,K}^i - x_{t-1,K}^i\|^2$, where t is the round index. For Strategy 3, it is $\|x_{t,K}^i - (x_{t,0}^i + \Delta_{t-1}^i)\|^2$. In (b) we measure the deviation of movement from the initial model in each round by cosine distance. For Strategy 2, it is $\langle \Delta_{t-1}^i, x_{t-1,K}^i - x_{t,0}^i \rangle$. For Strategy 3, it is $\langle \Delta_{t-1}^i, \Delta_{t-1}^i \rangle$. Both of the two measurements indicate that the model estimated by Strategy 3 is closer to the true model than that by Strategy 2, especially in the first and middle stages of training.

from the deterministic aggregation of all clients. To conquer this problem, the second strategy allows all clients in \mathcal{S}_t to take part in aggregation phase, even part of them skip local training:

Strategy 2 *If client i will skip round t , it returns the local model of the last round $x_{t-1,K}^i$ to the server instead of calculating $x_{t,K}^i$.*

This strategy is also presented by previous literatures such as [5, 8]. However, Strategy 2 uses stale local models, which reduces the performance of aggregated model.

To overcome the drawbacks of both strategies, the clients in \mathcal{S}_t should provide local models but without computationally intensive local training. Although it appears contradictory, it motivates us to "guess" a local model that is as close as possible to the model obtained by gradient iterations, but with negligible computational overhead. Indeed, Strategy 2 can be viewed as a model estimation, but the estimation is insufficiently precise, resulting in poor performance.

For client i , we observe the movement of the local model in round $t-1$ and get the moving vector $\Delta_{t-1}^i = x_{t-1,K}^i - x_{t-1,0}^i$. In the subsequent round t , we assume that the local model would do the same movement as before. Hence we have following strategy to estimate the local model:

Strategy 3 *If client i will skip round t , it returns the estimated local model $x_{t,0}^i + \Delta_{t-1}^i$ as $x_{t,K}^i$.*

Fig. 2 illustrates the effect of model estimation by both Euclidean distance and cosine distance. In Fig. 2(a) we illustrate the Euclidean distances between observed local models and the true model inferred by Eq. (2). For Strategy 2, the estimated model is the one obtained in the previous round. In Fig. 2(b) we measure the cosine distances between the moving vector from $x_{t,0}^i$ to estimated model and to the true model respectively. Both measures show that the model observed by Strategy 3 is close to the real one, and is better than that by Strategy 2 especially in the beginning and middle stages of training. Therefore, compared with Strategy 2, Strategy 3 is a better one to estimate the local model.

3.3 Method

Based on Strategy 3, we propose Computationally Customized Federated Learning (CCFL) illustrated in Algorithm 1. According to local computational resources, each client decides to either perform local training (line 7 to line 11) or estimate the local update (line 13). Actually, for client i with $p_i < 1$, more than one successive rounds may be skipped, leading to $\Delta_t^i = \Delta_{t-1}^i = \Delta_{t-2}^i = \dots$. The stale moving vectors may hurt the convergence of the method, which would be investigated later. If all clients have sufficient resources ($p_i = 1$), CCFL degrades to normal federated learning.

Algorithm 1 CCFL: Computationally Customized Federated Learning

```
1: Initialize  $x_0$ .
2: for  $t = 0$  to  $T - 1$  do
3:   Server selects  $\mathcal{S}_t$  randomly and sends  $x_t$  to clients in  $\mathcal{S}_t$ .
4:   (At client:)
5:   for each client  $i \in \mathcal{S}_t$  in parallel do
6:     if not skip this round then ▷ with probability  $p_i$ 
7:       initial local model:  $x_{t,0}^i = x_t$ .
8:       for  $k = 0$  to  $K - 1$  do
9:         Update local model by an unbiased estimate of gradient:  $x_{t,k+1}^i = x_{t,k}^i - \eta g_{t,k}^i$ .
10:      end for
11:      Get  $\Delta_t^i = x_{t,K}^i - x_{t,0}^i$ .
12:    else ▷ with probability  $1 - p_i$ 
13:      Get  $\Delta_t^i = \Delta_{t-1}^i$ .
14:    end if
15:    Send  $\Delta_t^i$  back to the server.
16:  end for
17:  (At server:)
18:   $\Delta_t = \frac{1}{|\mathcal{S}_t|} \sum_{i \in \mathcal{S}_t} \Delta_t^i$ .
19:  Update global model  $x_{t+1} = x_t + \Delta_t$ .
20: end for
```

Obviously, if the client skips one round by estimating the movement of the local model, there is almost no computational overhead compared with computation-consuming local training. Therefore, smaller p_i means lower computational cost in the training.

4 Theoretical Analysis

4.1 Convergence Analysis

In order to analyze the convergence of CCFL, we first state the assumptions as follows.

Assumption 1 (L-Lipschitz Continuous Gradient) *Function $f_i(x)$ is L -smooth, i.e., $\forall x, y \in \mathbb{R}^d$,*

$$\|\nabla f_i(y) - \nabla f_i(x)\| \leq L\|y - x\| \quad (4)$$

Assumption 2 (Unbiased Local Gradient Estimator) *For the i -th client, the local gradient estimator $g_{t,k}^i = \nabla f_i(x_{t,k}^i, \xi_{t,k}^i)$ is unbiased and the variance is bounded, where $\xi_{t,k}^i$ is a random mini-batch of local data in the k -th step of the t -th round at the i -th client, i.e.,*

$$\mathbb{E}[g_{t,k}^i] = \nabla f_i(x_{t,k}^i) \quad (5)$$

$$\|g_{t,k}^i - \nabla f_i(x_{t,k}^i)\|^2 \leq \sigma_L^2 \quad (6)$$

Assumption 3 (Bounded Global Variance) *The variance of local gradients with respect to the global gradient is bounded, i.e.,*

$$\mathbb{E}\|\nabla f_i(x) - \nabla f(x)\|^2 \leq \sigma_G^2. \quad (7)$$

Assumption 1 and 2 are standard in general non-convex optimization [31, 32, 33, 34]. Assumption 3 is also a common assumption in federated optimization [4, 35, 36], where σ_G is used to quantify the degree of data heterogeneity among clients. In particular, $\sigma_G = 0$ corresponds to IID (Independent Identically Distributed) data setting.

Based on the above assumptions, we present the theoretical results for the non-convex problem. For simplicity, we consider CCFL with full client participation, i.e. $|\mathcal{S}_t| = N$.

Theorem 1 *For N participants, suppose there are $r \cdot N$ clients ($r \in [0, 1]$) with insufficient computational resources, each of which performs local iterations at least in one round every W rounds*

($W \ll T$). If the local learning rate satisfies $\eta \leq \min(\frac{\sqrt{1+24r^2W^2L}-1}{12r^2KW^2L}, \frac{1}{\sqrt{60(6r^2+1)KL}})$, we have the following convergence result for CCFL:

$$\min_{t \in [T]} \|\nabla f(x_t)\|^2 \leq \frac{f(x_0) - f(x^*)}{c\eta KT} + \frac{D}{c\eta K}, \quad (8)$$

where

$$D = 5(6r^2 + 1)(\sigma_L^2 + 6K\sigma_G^2)L^2K^2\eta^3 + \frac{K\eta^2L}{2N}\sigma_L^2, \quad (9)$$

and c is a constant satisfying $0 < c < \frac{1}{2}$.

For client i , W is strongly related to p_i . If the client participates in FL in a round-robin manner, i.e., once per W rounds (“round-robin” schedule in Section 6.1), $p_i = \frac{1}{W}$. If the client participates at random, i.e., once randomly in W rounds (“ad-hoc” schedule in Section 6.1), $p_i = \mathbb{E}[\frac{1}{W}]$. As a result, we view $\frac{1}{W}$ as being equivalent to p_i by expectation.

With Theorem 1, we have the following convergence rate for CCFL with a proper choice learning rate:

Corollary 1 Let $\eta = \frac{\sqrt{N}}{\sqrt{TK}}$, then we have

$$\min_{t \in [T]} \|\nabla f(x_t)\|^2 = \mathcal{O}(\frac{1}{\sqrt{NKT}} + \frac{1}{T}). \quad (10)$$

From this corollary, the convergence rate of CCFL is the same as FedAvg, which is shown in [4].

4.2 Discussion

Compared to vanilla FedAvg, CCFL introduces two hyper-parameters r and W to describe clients with insufficient computational resources. Here we discuss the influence of them.

Influence of r . From the analysis we find r is not a critical factor for convergence rate. CCFL has the same order of convergence speed as FedAvg (both are $\mathcal{O}(\frac{1}{\sqrt{NKT}})$), even all the clients would skip the local training with a positive probability. However, r affects the magnitude of the coefficients, i.e., c . From Eq. (8) in Theorem 1, a larger c would accelerate the convergence (note that the order of convergence is not changed). From the proof of Theorem 1, $c < (\frac{1}{2} - (6r^2L^2 + L^2)\frac{H_2}{K})$. It can be drawn directly that a smaller M is corresponding to a larger c . Therefore, r has a moderate influence on the convergence rate of CCFL.

Influence of W . From the analysis we find W is not a critical factor for convergence rate. W is even not appear directly in the right side of Eq. (8). However, W affects the range of η . When W becomes larger, one of the upper bound of $\eta (\frac{\sqrt{1+24r^2W^2L}-1}{12r^2KW^2L})$ gets smaller. To make Eq. (8) hold, we should choose smaller η for larger W , which leads to a larger constant term of $\mathcal{O}(\frac{1}{\sqrt{T}})$. For example, suppose η decreases from $\frac{\sqrt{N}}{\sqrt{TK}}$ to $\frac{\sqrt{N}}{2\sqrt{TK}}$, the convergence rate is from Eq. (10) to

$$\min_{t \in [T]} \|\nabla f(x_t)\|^2 = \mathcal{O}(\frac{2}{\sqrt{NKT}} + \frac{1}{2\sqrt{NKT}} + \frac{1}{T}). \quad (11)$$

Intuitively, larger W leads to more stale local models. Smaller η can mitigate the influence of stale model. It matches the conclusion above. Therefore, W has a moderate influence on the convergence rate of CCFL.

5 Computation-Efficient FL

Here we discuss a special case of CCFL with $r = 1$ (denoted as CCFL($r = 1$)). In this case the number of each client performing local training reduces is decreased by W compared with traditional FedAvg. It indicates that we can reduce the overhead of traditional FL without sacrificing performance. Concretely, in each training round of FL, each participant executes local training with probability $1/W$ and estimates local model with probability $(1 - 1/W)$ (on the contrary, each participant executes

Table 1: Performance (top-1 validation accuracy) comparison on CIFAR-10 with different data heterogeneity, where $N = 8$ and $\beta = 4$.

	round-robin				ad-hoc			
	totally non-IID	90% non-IID	80% non-IID	IID	totally non-IID	90% non-IID	80% non-IID	IID
FedAvg	56.82	66.67	68.99	72.88	56.82	66.67	68.99	72.88
Strategy 1	30.79	55.18	61.35	69.46	39.45	60.16	63.95	71.95
Strategy 2	51.45	61.72	63.37	67.35	48.75	60.18	61.58	66.35
CCFL	56.28	65.79	67.84	72.43	55.94	66.41	68.61	72.53

local training with probability 1 for conventional FL). In fact, from this point of view, the field of application of CCFL is effectively broadened from addressing compute heterogeneity to any FL scenario. It improves the computation efficiency of traditional FL without any other overhead. It also be demonstrated in Section 6.5.

6 Experiments

6.1 Datasets and Experimental Settings

We investigate CCFL on 3 datasets and corresponding models as follows:

- **CIFAR-10** [37]. CIFAR-10 is made up of 60000 32x32 color pictures divided into ten categories, each containing 6000 images. The training set has 50000 photos, whereas the test set has 10000 images. We use a CNN network with 2 convolutional-pooling layers and 3 fully connected layers (abbr. CNN), and ResNet-18 on CIFAR-10.
- **FMNIST** [38]. Fashion-MNIST is an upgraded version of MNIST. The task’s complexity has risen as compared to MNIST. It contains gray-scale photos of 70000 fashion goods from 10 categories in 28x28 dimensions. There are 7000 photos in each category. The training set has 60000 photos, whereas the test set has 10000 ones. For FMNIST, we utilize a multi-layered perception network with 3 fully connected layers (abbr. MLP).
- **CIFAR-100** [37]. CIFAR-100 is divided into 100 classes, each including 500 images for training and 100 images for testing. For this dataset, We employ ResNet-18 with group normalization as default.

We evaluate the proposed CCFL on tasks involving the customization of computational resources. To facilitate our discussion, we assume a specific heterogeneous training budget with an imbalanced resource distribution among clients. Specifically, for the i -th client, $p_i = (1/2)^{\lfloor \frac{\beta-i}{N} \rfloor}$, where β controls the number of heterogeneous resource types. The corresponding r is about $1 - \frac{1}{\beta}$, since there are $\lceil \frac{N}{\beta} \rceil$ clients with $p_i = 1$. For instance, if we set $\beta = 3$, all the clients are equally divided into 3 groups in which the clients contribute 1, 0.5 and 0.25 times of maximum computational resource for training, respectively.

For the client with $p_i < 1$, we consider two types of scheduling methods to saving the computational resources. The first is “round-robin” schedule, where client i skips $(1/p_i - 1)$ rounds and performs SGD in one round every $1/p_i$ rounds strictly. This schedule simulates the situation that the client can schedule tasks in advance. For example, if the client has insufficient energy, it can plan the rounds ahead of time to guarantee that it has enough battery to endure until the end of training. The second is “ad-hoc” schedule, in which client i skips SGD iterations in the current round with the probability $1 - p_i$. This schedule models the situation that computational resources vary randomly throughout training, for example due to the addition and removal of other tasks.

6.2 Performance

Table 1 compares the accuracy of CCFL and other two strategies in cross-silo setting. We construct a variety of federated scenarios containing 8 clients on CIFAR-10 with different data heterogeneity

Table 2: Performance (top-1 validation accuracy) comparison on FMNIST with different data heterogeneity, where $N = 100$ and $\beta = 4$. The classes of training data are randomly distributed across clients with different computational resources.

	10%	20%	30%	40%
FedAvg	78.76 \pm 2.62	80.52 \pm 1.66	82.44 \pm 0.73	82.48 \pm 0.58
Strategy 1	60.12 \pm 12.51	74.61 \pm 4.79	78.90 \pm 2.65	80.61 \pm 0.82
Strategy 2	66.58 \pm 3.66	73.63 \pm 3.86	77.76 \pm 1.61	78.91 \pm 0.70
CCFL	75.78\pm2.30	78.40\pm2.50	81.70\pm 0.81	81.42\pm0.31

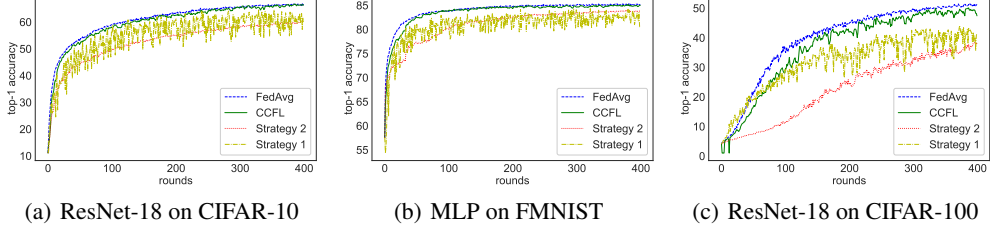


Figure 3: Performance comparison on multiple datasets.

following [17]. We use CNN model, and use SGD as local optimizer with learning rate 0.01. FL methods perform 400 rounds, and 3 epochs in each round. To simulate heterogeneous computational resources, we set $\beta = 4$, i.e., the clients are on 4 different levels based on the sufficiency of the computational resources, performing local training with probabilities 1, 0.5, 0.25, 0.125, respectively. We investigate the model performance on both “round-robin” schedule and “ad-hoc” schedule. The result shows that CCFL outperforms the other two strategies regardless of data heterogeneity and task schedules. Remarkably, compared to **FedAvg without the limitation of computational resources that all clients participate in training every round (in the following we name this baseline as FedAvg for short)**, CCFL reaches a similar level of performance, even though 75% clients are not fully involved, and 25% clients participate in only 1/8 of the training rounds. Fig. 6 in Section A.4 visualizes the participation of the clients. Compared with FedAvg, CCFL requires much less computational resources. Furthermore, CCFL performs similarly in the two schedules. Without loss of generality, in the following we set “ad-hoc” schedule as default.

To compare the accuracy of CCFL and other two strategies in cross-device setting, we construct federated scenarios on FMNIST with 100 clients and varying participant ratios in each round (from 10% to 40%). Each client contains two classes of training data. We specify $\beta = 4$. All methods run 400 rounds with 200 iterations in each round. Fig. 7 in Section A.4 visualizes the participation of the clients. In Table 2, where clients are randomly selected, the model performances gradually become stable as the proportion of participants per round increases. CCFL performs comparable to FedAvg, with a performance decline of no more than 3%, and consistently outperforms two other strategies. Furthermore, CCFL is as consistent as FedAvg. On the contrary, the performances of models training by other two methods fluctuate more, especially with small participant ratios (e.g., 10%).

6.3 Convergence

We compare the convergence curves of CCFL and FedAvg as well as other two baselines on three datasets in Fig. 3. We construct the scenarios with 8 clients and $\beta=4$ under 90% non-IID data setting. CCFL exhibits convergence curves that are almost identical to FedAvg, especially on two simpler datasets (FMNIST and CIFAR-10). It means that with CCFL the model training process is almost no interference from computational underpower. It also verifies Corollary 1 that CCFL has the same convergence rate as FedAvg. On the contrary, Strategy 1 performs very unstable that the curves wobble a lot. Strategy 2 has a stable convergence curve, but it is significantly lower than FedAvg and CCFL.

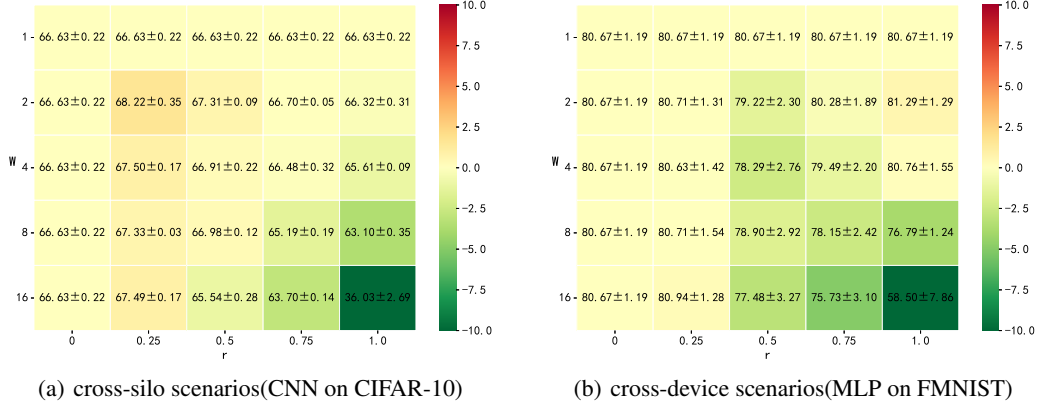


Figure 4: Performance changes with varying of r and W (CCFL). The color at each grid indicates the performance difference between the model of CCFL with corresponding r and W and FedAvg (i.e., CCF with $r = 0$ or $W = 0$).

6.4 Factors of CCFL

To understand the effect of key factors of CCFL, namely r and W , we construct federated scenarios in which clients with insufficient computational resources have the same W . Because the “round-robin” scheme and the “ad-hoc” scheme perform similarly, we choose the “ad-hoc” scheme for the sake of generalization, and set the corresponding $p_i = \frac{1}{W}$. Particularly, CCFL is degraded into FedAvg when $W = 1$ or $r = 0$.

Fig. 4 demonstrates the model performance by gridding the values of r and W . With the increment of W or r , the performance is essentially steady, unless both r and W are extremely large. Fig. 4(a) illustrates the performances in cross-silo scenarios, where CCFL even surpasses FedAvg while requiring less computing effort for some circumstances (e.g., $r = 0.25$). It indicates that excessive computing resources (full participation in each round) are not necessarily beneficial to accelerate the training. The same phenomenon does not appear in Fig. 4(b), where only 20% clients participate in training in each round. In both figures, when $r = 1.0$ and $W = 16$ the model performance of CCFL degrades significantly even more than that of Strategy 1 and Strategy 2 (in Fig. 8 and Fig. 9 in A.6). In this situation, each client executes local training only once about every 16 rounds. The uploaded local models in most rounds are quite inaccurate since they are guessed based on outdated information. When r or W are reduced, the performance of CCFL rapidly improves since more accurate information is introduced.

6.5 Computational Efficiency Improvement

We compare the performance of CCFL($r = 1$) with FedAvg under the same computation overhead. Specifically, for each participant in CCFL($r = 1$), the number of rounds to perform local training is only $1/W$ of corresponding FedAvg. Therefore, to compare both methods with the same computational budgets, we compare the performance of CCFL($r = 1$) (and the number of training round T) and FedAvg with total training round T/W . We demonstrate the comparison both under cross-silo (as Fig. 4(a)) and cross-device (as Fig. 4(b)) settings. When W is moderate large (e.g., $W \leq 8$), CCFL($r = 1$) outperforms FedAvg. However, when W is too large (e.g., $W = 8$), CCFL underperforms FedAvg, because the local estimations are far from the true models. Therefore, we cannot enlarge W without an upper limit.

7 Conclusion

In this paper, we present a strategy for estimating local models with little computational overhead. Based on it, we propose a novel federated learning method CCFL for customizing computational resources to address the challenge of computation heterogeneity. Both theoretical analysis and

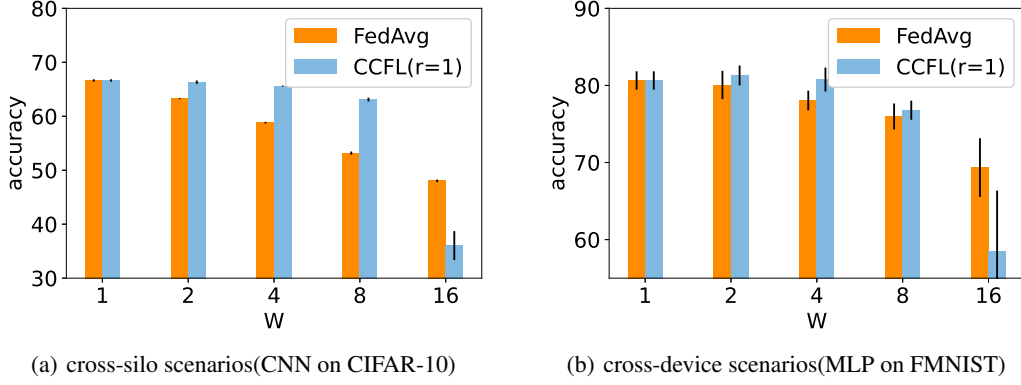


Figure 5: Efficiency comparison between CCFL($r = 1$) with FedAvg.

extensive experiments demonstrate the effectiveness of CCFL. Meanwhile, CCFL can be viewed as a computation-efficient extension of FedAvg that it can replace FedAvg in any scenarios without aiming to tackle computation heterogeneity.

References

- [1] Brendan McMahan, Eider Moore, Daniel Ramage, Seth Hampson, and Blaise Agüera y Arcas. Communication-efficient learning of deep networks from decentralized data. In *Artificial intelligence and statistics*, pages 1273–1282. PMLR, 2017.
- [2] Peter Kairouz, H Brendan McMahan, Brendan Avent, Aurélien Bellet, Mehdi Bennis, Arjun Nitin Bhagoji, Kallista Bonawitz, Zachary Charles, Graham Cormode, Rachel Cummings, et al. Advances and open problems in federated learning. *Foundations and Trends® in Machine Learning*, 14(1–2):1–210, 2021.
- [3] Sashank J Reddi, Zachary Charles, Manzil Zaheer, Zachary Garrett, Keith Rush, Jakub Konečný, Sanjiv Kumar, and Hugh Brendan McMahan. Adaptive federated optimization. In *International Conference on Learning Representations*, 2020.
- [4] Haibo Yang, Minghong Fang, and Jia Liu. Achieving linear speedup with partial worker participation in non-IID federated learning. In *International Conference on Learning Representations*, 2021.
- [5] Yikai Yan, Chaoyue Niu, Yucheng Ding, Zhenzhe Zheng, Fan Wu, Guihai Chen, Shaojie Tang, and Zhihua Wu. Distributed non-convex optimization with sublinear speedup under intermittent client availability. *arXiv preprint arXiv:2002.07399*, 2020.
- [6] Fan Lai, Yinwei Dai, Sanjay Singapuram, Jiachen Liu, Xiangfeng Zhu, Harsha Madhyastha, and Mosharaf Chowdhury. FedScale: Benchmarking model and system performance of federated learning at scale. In *International Conference on Machine Learning*, pages 11814–11827. PMLR, 2022.
- [7] Heqiang Wang and Jie Xu. Friends to help: Saving federated learning from client dropout. *arXiv preprint arXiv:2205.13222*, 2022.
- [8] Xinran Gu, Kaixuan Huang, Jingzhao Zhang, and Longbo Huang. Fast federated learning in the presence of arbitrary device unavailability. *Advances in Neural Information Processing Systems*, 34:12052–12064, 2021.
- [9] Yann Fraboni, Richard Vidal, Laetitia Kameni, and Marco Lorenzi. Clustered sampling: Low-variance and improved representativity for clients selection in federated learning. In *International Conference on Machine Learning*, pages 3407–3416. PMLR, 2021.

- [10] Yue Zhao, Meng Li, Liangzhen Lai, Naveen Suda, Damon Civin, and Vikas Chandra. Federated learning with non-iid data. *arXiv preprint arXiv:1806.00582*, 2018.
- [11] Sai Praneeth Karimireddy, Satyen Kale, Mehryar Mohri, Sashank Reddi, Sebastian Stich, and Ananda Theertha Suresh. Scaffold: Stochastic controlled averaging for federated learning. In *International Conference on Machine Learning*, pages 5132–5143. PMLR, 2020.
- [12] Xianfeng Liang, Shuheng Shen, Jingchang Liu, Zhen Pan, Enhong Chen, and Yifei Cheng. Variance reduced local sgd with lower communication complexity. *arXiv preprint arXiv:1912.12844*, 2019.
- [13] Sai Praneeth Karimireddy, Martin Jaggi, Satyen Kale, Mehryar Mohri, Sashank Reddi, Sebastian U Stich, and Ananda Theertha Suresh. Breaking the centralized barrier for cross-device federated learning. *Advances in Neural Information Processing Systems*, 34:28663–28676, 2021.
- [14] Tian Li, Anit Kumar Sahu, Manzil Zaheer, Maziar Sanjabi, Ameet Talwalkar, and Virginia Smith. Federated optimization in heterogeneous networks. *arXiv preprint arXiv:1812.06127*, 2018.
- [15] Xin Yao, Tianchi Huang, Chenglei Wu, Rui-Xiao Zhang, and Lifeng Sun. Federated learning with additional mechanisms on clients to reduce communication costs. *arXiv preprint arXiv:1908.05891*, 2019.
- [16] Qinbin Li, Bingsheng He, and Dawn Song. Model-contrastive federated learning. In *Proceedings of the IEEE/CVF Conference on Computer Vision and Pattern Recognition*, pages 10713–10722, 2021.
- [17] Hao Zhang, Tingting Wu, Siyao Cheng, and Jie Liu. Fedcos: A scene-adaptive enhancement for federated learning. *IEEE Internet of Things Journal*, 2022.
- [18] Enmao Diao, Jie Ding, and Vahid Tarokh. Heterofl: Computation and communication efficient federated learning for heterogeneous clients. In *International Conference on Learning Representations*, 2021.
- [19] Samuel Horvath, Stefanos Laskaridis, Mario Almeida, Ilias Leontiadis, Stylianos Venieris, and Nicholas Lane. Fjord: Fair and accurate federated learning under heterogeneous targets with ordered dropout. *Advances in Neural Information Processing Systems*, 34:12876–12889, 2021.
- [20] Junyuan Hong, Haotao Wang, Zhangyang Wang, and Jiayu Zhou. Efficient split-mix federated learning for on-demand and in-situ customization. In *International Conference on Learning Representations*, 2022.
- [21] Yiqun Mei, Pengfei Guo, Mo Zhou, and Vishal Patel. Resource-adaptive federated learning with all-in-one neural composition. In Alice H. Oh, Alekh Agarwal, Danielle Belgrave, and Kyunghyun Cho, editors, *Advances in Neural Information Processing Systems*, 2022.
- [22] Takayuki Nishio and Ryo Yonetani. Client selection for federated learning with heterogeneous resources in mobile edge. In *ICC 2019-2019 IEEE international conference on communications (ICC)*, pages 1–7. IEEE, 2019.
- [23] Tao Lin, Lingjing Kong, Sebastian U Stich, and Martin Jaggi. Ensemble distillation for robust model fusion in federated learning. *Advances in Neural Information Processing Systems*, 33:2351–2363, 2020.
- [24] Yanlin Zhou, George Pu, Xiyao Ma, Xiaolin Li, and Dapeng Wu. Distilled one-shot federated learning. *arXiv preprint arXiv:2009.07999*, 2020.
- [25] Bing Luo, Xiang Li, Shiqiang Wang, Jianwei Huang, and Leandros Tassioulas. Cost-effective federated learning design. In *IEEE INFOCOM 2021-IEEE Conference on Computer Communications*, pages 1–10. IEEE, 2021.
- [26] Jianyu Wang and Gauri Joshi. Adaptive communication strategies to achieve the best error-runtime trade-off in local-update sgd. *Proceedings of Machine Learning and Systems*, 1:212–229, 2019.

- [27] Amna Arouj and Ahmed M Abdelmoniem. Towards energy-aware federated learning on battery-powered clients. In *Proceedings of the 1st ACM Workshop on Data Privacy and Federated Learning Technologies for Mobile Edge Network*, pages 7–12, 2022.
- [28] Young Geun Kim and Carole-Jean Wu. Autofl: Enabling heterogeneity-aware energy efficient federated learning. In *MICRO-54: 54th Annual IEEE/ACM International Symposium on Microarchitecture*, pages 183–198, 2021.
- [29] WANG Luping, WANG Wei, and LI Bo. Cmfl: Mitigating communication overhead for federated learning. In *2019 IEEE 39th international conference on distributed computing systems (ICDCS)*, pages 954–964. IEEE, 2019.
- [30] Durmus Alp Emre Acar, Yue Zhao, Ramon Matas, Matthew Mattina, Paul Whatmough, and Venkatesh Saligrama. Federated learning based on dynamic regularization. In *International Conference on Learning Representations*, 2021.
- [31] Jorge Nocedal. Optimization methods for large-scale machine learning. *Siam Review*, 60(2), 2016.
- [32] Jianyu Wang, Zachary Charles, Zheng Xu, Gauri Joshi, H Brendan McMahan, Maruan Al-Shedivat, Galen Andrew, Salman Avestimehr, Katharine Daly, Deepesh Data, et al. A field guide to federated optimization. *arXiv preprint arXiv:2107.06917*, 2021.
- [33] Farzin Haddadpour and Mehrdad Mahdavi. On the convergence of local descent methods in federated learning. *arXiv preprint arXiv:1910.14425*, 2019.
- [34] Dong Yin, Ashwin Pananjady, Max Lam, Dimitris Papailiopoulos, Kannan Ramchandran, and Peter Bartlett. Gradient diversity: a key ingredient for scalable distributed learning. In *International Conference on Artificial Intelligence and Statistics*, pages 1998–2007. PMLR, 2018.
- [35] Sashank J. Reddi, Zachary Charles, Manzil Zaheer, Zachary Garrett, Keith Rush, Jakub Konečný, Sanjiv Kumar, and Hugh Brendan McMahan. Adaptive federated optimization. In *International Conference on Learning Representations*, 2021.
- [36] Shuheng Shen, Linli Xu, Jingchang Liu, Xianfeng Liang, and Yifei Cheng. Faster distributed deep net training: Computation and communication decoupled stochastic gradient descent. In *Proceedings of the Twenty-Eighth International Joint Conference on Artificial Intelligence*, pages 4582–4589, 7 2019.
- [37] A Krizhevsky. Learning multiple layers of features from tiny images. *Master’s thesis, University of Tront*, 2009.
- [38] Han Xiao, Kashif Rasul, and Roland Vollgraf. Fashion-mnist: a novel image dataset for benchmarking machine learning algorithms. *arXiv preprint arXiv:1708.07747*, 2017.

A Appendix

A.1 Variants of CCFL

In Algorithm 1 each client saves Δ_i^t for further use after performing line 13, which leads to extra storage cost. Actually, since the server knows Δ_{t-1}^i if the historical information is saved, the server does not need the client to return the estimated movement of the local model. Instead, the server can perform line 13 directly when it knows the corresponding client would skip this round (for example, the client returns a “skip” signal if it would skip the round). In this situation, the overhead of clients is further reduced: besides reducing the computational overhead, both the storage overhead and communication overhead are reduced. Specifically, the storage of Δ_{t-1}^i is transferred to the server. The amount of data being transmitted is reduced from thousands of even millions of bytes (determined by the number of model parameters) to at least 1 bit (indicating “skip” or not). We propose other variant of CCFL (Algorithm 2) without increasing the storage overhead of clients. Furthermore, the two schemes that the historical information is stored locally or on the server can

be mixed to obtain the third variant of CCFL (Algorithm 3). For the client with sufficient storage and good communication conditions, the historical information can be saved by the client itself and performs CCFL as Algorithm 1, otherwise the historical information is saved by the server. By this hybrid scheme, we can balance the local requirement and the server load. After all, it is also a great burden to the server if all the local historical information is stored on the server.

Algorithm 2 CCFL: Computationally Customized Federated Learning (historical information backup on the server)

```

1: Initialize  $x_0$ .
2: for  $t = 0$  to  $T - 1$  do
3:   Server selects  $\mathcal{S}_t$  randomly and sends  $x_t$  to clients in  $\mathcal{S}_t$ .
4:   (At client:)
5:   for each client  $i \in \mathcal{S}_t$  in parallel do
6:     if not skip this round then ▷ with probability  $p_i$ 
7:       initial local model:  $x_{t,0}^i = x_t$ .
8:       for  $k = 0$  to  $K - 1$  do
9:         Update local model by an unbiased estimate of gradient:  $x_{t,k+1}^i = x_{t,k}^i - \eta g_{t,k}^i$ .
10:      end for
11:      Get  $\Delta_t^i = x_{t,K}^i - x_{t,0}^i$ .
12:      Send  $\Delta_t^i$  back to the server.
13:    else ▷ with probability  $1 - p_i$ 
14:      Send ( $i$ , “skip” signal) to the server.
15:    end if
16:  end for
17:  (At server:)
18:  if Receive ( $i$ , “skip” signal) then
19:    Get  $\Delta_t^i = \Delta_{t-1}^i$ .
20:  end if
21:   $\Delta_t = \frac{1}{|\mathcal{S}_t|} \sum_{i \in \mathcal{S}_t} \Delta_t^i$ .
22:  Update global model  $x_{t+1} = x_t + \Delta_t$ .
23: end for

```

A.2 Important Lemmas

To understand Theorem 1 better, we list some important Lemmas here.

Lemma 1 For learning rate $\eta \leq \frac{1}{4LK}$, we have

$$\sum_{k=0}^{K-1} \mathbb{E} \|x_{t,k}^i - x_t\|^2 \leq 5K^2\eta^2\sigma_L^2 + 30K^3\eta^2\sigma_G^2 + 30K^3\eta^2\|\nabla f(x_t)\|^2. \quad (12)$$

Algorithm 3 CCFL: Computationally Customized Federated Learning (mixed backup of historical information)

```

1: Initialize  $x_0$ .
2: for  $t = 0$  to  $T - 1$  do
3:   Server selects  $\mathcal{S}_t$  randomly and sends  $x_t$  to clients in  $\mathcal{S}_t$ .
4:   (At client:)
5:   for each client  $i \in \mathcal{S}_t$  in parallel do
6:     if not skip this round then ▷ with probability  $p_i$ 
7:       initial local model:  $x_{t,0}^i = x_t$ .
8:       for  $k = 0$  to  $K - 1$  do
9:         Update local model by an unbiased estimate of gradient:  $x_{t,k+1}^i = x_{t,k}^i - \eta g_{t,k}^i$ .
10:      end for
11:      Get  $\Delta_t^i = x_{t,K}^i - x_{t,0}^i$ .
12:      Send  $\Delta_t^i$  back to the server.
13:    else ▷ with probability  $1 - p_i$ 
14:      if  $\Delta_{t-1}^i$  is backed up locally then
15:        Get  $\Delta_t^i = \Delta_{t-1}^i$ .
16:        Send  $\Delta_t^i$  back to the server.
17:      else
18:        Send ( $i$ , “skip” signal) to the server.
19:      end if
20:    end if
21:  end for
22:  (At server:)
23:  if Receive ( $i$ , “skip” signal) then
24:    Get  $\Delta_t^i = \Delta_{t-1}^i$ .
25:  end if
26:   $\Delta_t = \frac{1}{|\mathcal{S}_t|} \sum_{i \in \mathcal{S}_t} \Delta_t^i$ .
27:  Update global model  $x_{t+1} = x_t + \Delta_t$ .
28: end for

```

Proof 1

$$\begin{aligned}
& \mathbb{E} \|x_{t,k}^i - x_t\|^2 = \mathbb{E} \|x_{t,k-1}^i - \eta g_{t,k-1}^i - x_t\|^2 \\
& \leq \mathbb{E} \left\| \underbrace{x_{t,k-1}^i - x_t}_a - \underbrace{\eta(g_{t,k-1}^i - \nabla f_i(x_{t,k-1}^i))}_b + \underbrace{\nabla f_i(x_{t,k-1}^i) - \nabla f_i(x_t)}_c \right\|^2 \\
& \quad + \underbrace{\|\nabla f_i(x_t) - \nabla f(x_t)\|}_d + \underbrace{\|\nabla f(x_t)\|}_e \|^2 \\
& \stackrel{(a_1)}{=} \mathbb{E} \|a - \eta(c + d + e)\|^2 + \eta^2 \mathbb{E} \|b\|^2 \\
& \stackrel{(a_2)}{\leq} \left(1 + \frac{1}{2K-1}\right) \eta^2 \mathbb{E} \|a\|^2 + \eta^2 \mathbb{E} \|b\|^2 + 2\eta^2 K (3\mathbb{E} \|c\|^2 + 3\mathbb{E} \|d\|^2 + 3\mathbb{E} \|e\|^2) \\
& \stackrel{(a_3)}{\leq} \left(1 + \frac{1}{2K-1}\right) \eta^2 \mathbb{E} \|x_{t,k-1}^i - x_t\|^2 + \eta^2 \sigma_L^2 \\
& \quad + 6KL^2 \eta^2 \mathbb{E} \|x_{t,k-1}^i - x_t\|^2 + 6K\eta^2 \sigma_G^2 + 6K\eta^2 \|\nabla f(x_t)\|^2 \\
& = \left(1 + \frac{1}{2K-1} + 6KL^2 \eta^2\right) \mathbb{E} \|x_{t,k-1}^i - x_t\|^2 + \eta^2 \sigma_L^2 + 6K\eta^2 \sigma_G^2 + 6K\eta^2 \|\nabla f(x_t)\|^2 \\
& \stackrel{(a_4)}{\leq} \left(1 + \frac{1}{K-1}\right) \mathbb{E} \|x_{t,k-1}^i - x_t\|^2 + \eta^2 \sigma_L^2 + 6K\eta^2 \sigma_G^2 + 6K\eta^2 \|\nabla f(x_t)\|^2 \\
& \leq (K-1) \left[\left(1 + \frac{1}{K-1}\right)^k - 1\right] (\eta^2 \sigma_L^2 + 6K\eta^2 \sigma_G^2 + 6K\eta^2 \|\nabla f(x_t)\|^2),
\end{aligned} \tag{13}$$

where (a_1) follows Eq.(5), (a_2) follows $\|a+b\|^2 \leq (1+\gamma)\|a\|^2 + (1+\gamma^{-1})\|b\|^2$ and $\|\sum_{i=1}^n a_i\|^2 \leq n \sum_{i=1}^n \|a_i\|^2$, (a_3) follows Eq.(6), Eq.(4) and Eq.(7), (a_4) follows $\eta \leq \frac{1}{4LK}$. Thus,

$$\begin{aligned}
& \sum_{k=0}^{K-1} \mathbb{E} \|x_{t,k}^i - x_t\|^2 \\
& \leq \sum_{k=0}^{K-1} (K-1) \left[\left(1 + \frac{1}{K-1}\right)^k - 1 \right] (K-1) (\eta^2 \sigma_L^2 + 6K\eta^2 \sigma_G^2 + 6K\eta^2 \|\nabla f(x_t)\|^2) \quad (14) \\
& \stackrel{(a_5)}{\leq} 5K^2 (\eta^2 \sigma_L^2 + 6K\eta^2 \sigma_G^2 + 6K\eta^2 \|\nabla f(x_t)\|^2) \\
& = H_1 + H_2 \|\nabla f(x_t)\|^2
\end{aligned}$$

where (a_5) follows $(1 + \frac{1}{K-1})^K \leq 5$,

$$\begin{aligned}
H_1 &= 5K^2 \eta^2 \sigma_L^2 + 30K^3 \eta^2 \sigma_G^2 \\
H_2 &= 30K^3 \eta^2.
\end{aligned} \quad (15)$$

For convenient we denote $M = r \cdot N$. Suppose in round t , there are up to M clients skipping the iterations (since M can be selected from the whole rounds, we ignore the subscript t and regard it as a constant for simplicity), i.e. they perform line 13 in Algorithm 1. Moreover, the clients that continuously skip iterations exist. Without loss of generality, we suppose \mathcal{M}_j ($0 \leq j \leq W$) denotes the client set in which the clients have continuously skipped j rounds of local iteration. For instance, for the client i in \mathcal{M}_2 , it means $\Delta_t^i = \Delta_{t-1}^i = \Delta_{t-2}^i$. Particularly, the clients in \mathcal{M}_0 performs local SGD iterations in this round. Obviously, $\forall i \neq j, \mathcal{M}_i \cap \mathcal{M}_j = \emptyset$. Suppose $m_j = \mathbb{E}_t |\mathcal{M}_j|$ ($0 \leq j \leq W$) (for the clients, if the probability of skipping training are the same for each round, m_j is a constant in expectation), it has $\sum_{j=0}^W m_j = N$ and $\sum_{j=1}^W m_j = M$. Based on this condition, we have

$$\Delta_t = \frac{1}{N} \sum_i \Delta_t^i = \frac{1}{N} \sum_{j=0}^W \sum_{i \in \mathcal{M}_j} \Delta_{t-j}^i = -\frac{1}{N} \sum_{j=0}^W \sum_{i \in \mathcal{M}_j} \sum_{k=0}^{K-1} \eta g_{t-j,k}^i. \quad (16)$$

Lemma 2 For the moving vector of global model Δ_t , we have

$$\mathbb{E} \|\Delta_t\|^2 \leq \|\mathbb{E}[\Delta_t]\|^2 + \frac{K\eta^2}{N} \sigma_L^2. \quad (17)$$

Proof 2

$$\mathbb{E}[\Delta_t] = -\frac{1}{N} \sum_{j=0}^W \sum_{i \in \mathcal{M}_j} \sum_{k=0}^{K-1} \eta \nabla f_i(x_{t-j,k}^i), \quad (18)$$

Thus

$$\begin{aligned}
\mathbb{E} \|\Delta_t\|^2 &= \mathbb{E} \|\Delta_t - \mathbb{E}[\Delta_t] + \mathbb{E}[\Delta_t]\|^2 = \mathbb{E} \|\mathbb{E}[\Delta_t]\|^2 + \mathbb{E} \|\Delta_t - \mathbb{E}[\Delta_t]\|^2 \\
&= \|\mathbb{E}[\Delta_t]\|^2 + \mathbb{E} \left\| \frac{1}{N} \sum_{j=0}^W \sum_{i \in \mathcal{M}_j} \sum_{k=0}^{K-1} \eta (\nabla f_i(x_{t-j,k}^i) - g_{t-j,k}^i) \right\|^2 \quad (19) \\
&\leq \|\mathbb{E}[\Delta_t]\|^2 + \frac{K\eta^2}{N} \sigma_L^2.
\end{aligned}$$

A.3 Proof of Theorem 1

Proof 3 For the t -th round,

$$\begin{aligned}
\mathbb{E}[f(x_{t+1})] &\leq f(x_t) + \langle \nabla f(x_t), \mathbb{E}[x_{t+1} - x_t] \rangle + \frac{L}{2} \mathbb{E} \|x_{t+1} - x_t\|^2 \\
&\stackrel{(a)}{=} f(x_t) + \langle \nabla f(x_t), \mathbb{E}[\Delta_t + \eta K \nabla f(x_t) - \eta K \nabla f(x_t)] \rangle + \frac{L}{2} \mathbb{E} \|\Delta_t\|^2 \quad (20) \\
&= f(x_t) - \eta K \|\nabla f(x_t)\|^2 + \underbrace{\langle \nabla f(x_t), \mathbb{E}[\Delta_t] + \eta K \nabla f(x_t) \rangle}_{A_1} + \frac{L}{2} \mathbb{E} \|\Delta_t\|^2.
\end{aligned}$$

The term A_1 can be bounded as follows

$$\begin{aligned}
A_1 &= \langle \sqrt{\eta K} \nabla f(x_t), \frac{1}{\sqrt{\eta K}} \mathbb{E}[\Delta_t] + \sqrt{\eta K} \nabla f(x_t) \rangle \\
&\stackrel{(a_1)}{=} \frac{\eta K}{2} \|\nabla f(x_t)\|^2 + \frac{1}{2\eta K} \|\mathbb{E}[\Delta_t] + \eta K \nabla f(x_t)\|^2 - \frac{1}{2\eta K} \|\mathbb{E}[\Delta_t]\|^2
\end{aligned} \tag{21}$$

where (a_1) follows $2\langle a, b \rangle = \|a\|^2 + \|b\|^2 - \|a - b\|^2$. Thus

$$\begin{aligned}
\mathbb{E}[f(x_{t+1})] &\leq f(x_t) - \frac{\eta K}{2} \|\nabla f(x_t)\|^2 + \frac{1}{2\eta K} \|\mathbb{E}[\Delta_t] + \eta K \nabla f(x_t)\|^2 \\
&\quad + \frac{L}{2} \mathbb{E}\|\Delta_t\|^2 - \frac{1}{2\eta K} \|\mathbb{E}[\Delta_t]\|^2 \\
&\leq f(x_t) - \frac{\eta K}{2} \|\nabla f(x_t)\|^2 + \underbrace{\frac{1}{2\eta K} \|\mathbb{E}[\Delta_t] + \eta K \nabla f(x_t)\|^2}_{A_2} \\
&\quad + \frac{K\eta^2 L}{2N} \sigma_L^2 - \left(\frac{1}{2\eta K} - \frac{L}{2}\right) \|\mathbb{E}[\Delta_t]\|^2
\end{aligned} \tag{22}$$

For A_2 :

$$\begin{aligned}
&\frac{1}{2\eta K} \|\mathbb{E}[\Delta_t] + \eta K \nabla f(x_t)\|^2 \\
&= \frac{1}{2\eta K} \left\| -\frac{\eta}{N} \sum_{i=1}^N \sum_{k=0}^{K-1} \nabla f_i(x_{t,k}^i) + \frac{\eta}{N} \sum_{j=1}^W \sum_{i \in \mathcal{M}_j} \sum_{k=0}^{K-1} (\nabla f_i(x_{t,k}^i) - \nabla f_i(x_{t-j,k}^i)) \right. \\
&\quad \left. + \frac{\eta}{N} \sum_{i=1}^N \sum_{k=0}^{K-1} \nabla f_i(x_t) \right\|^2 \\
&\stackrel{(a_2)}{\leq} \underbrace{\frac{\eta}{K} \left\| \frac{1}{N} \sum_{j=1}^W \sum_{i \in \mathcal{M}_j} \sum_{k=0}^{K-1} (\nabla f_i(x_{t,k}^i) - \nabla f_i(x_{t-j,k}^i)) \right\|^2}_B \\
&\quad + \underbrace{\frac{\eta}{K} \left\| \frac{1}{N} \sum_{i=1}^N \sum_{k=0}^{K-1} \nabla f_i(x_{t,k}^i) - \frac{1}{N} \sum_{i=1}^N \sum_{k=0}^{K-1} \nabla f_i(x_t) \right\|^2}_C
\end{aligned} \tag{23}$$

where (a_2) follows $\|a + b\|^2 \leq 2\|a\|^2 + 2\|b\|^2$,

The term B is bounded as

$$\begin{aligned}
B &= \frac{\eta}{K} \left\| \frac{1}{N} \sum_{j=1}^W \sum_{i \in \mathcal{M}_j} \sum_{k=0}^{K-1} (\nabla f_i(x_{t,k}^i) - \nabla f_i(x_{t-j,k}^i)) \right\|^2 \\
&\stackrel{(b_1)}{\leq} \frac{M\eta}{N^2} \sum_{j=1}^W \sum_{i \in \mathcal{M}_j} \sum_{k=0}^{K-1} \left\| (\nabla f_i(x_{t,k}^i) - \nabla f_i(x_{t-j,k}^i)) \right\|^2 \\
&\stackrel{(b_2)}{\leq} \frac{M\eta L^2}{N^2} \sum_{j=1}^W \sum_{i \in \mathcal{M}_j} \sum_{k=0}^{K-1} \|x_{t,k}^i - x_{t-j,k}^i\|^2 \\
&\stackrel{(b_3)}{\leq} \frac{3M\eta L^2}{N^2} \left(\underbrace{\sum_{j=1}^W \sum_{i \in \mathcal{M}_j} \sum_{k=0}^{K-1} \|x_{t,k}^i - x_t\|^2}_{B_1} + \underbrace{\sum_{j=1}^W \sum_{i \in \mathcal{M}_j} \sum_{k=0}^{K-1} \|x_t - x_{t-j}\|^2}_{B_2} \right. \\
&\quad \left. + \underbrace{\sum_{j=1}^W \sum_{i \in \mathcal{M}_j} \sum_{k=0}^{K-1} \|x_{t-j,k}^i - x_{t-j}\|^2}_{B_3} \right)
\end{aligned} \tag{24}$$

where (b_1) and (b_3) follow $\|\sum_{i=1}^n a_i\|^2 \leq n \sum_{i=1}^n \|a_i\|^2$, (b_2) follows Assumption 1.

For the three items B_1 , B_2 and B_3 ,

$$B_1 = \sum_{j=1}^W \sum_{i \in \mathcal{M}_j} \sum_{k=0}^{K-1} \|x_{t,k}^i - x_t\|^2 \leq M(H_1 + H_2 \|\nabla f(x_t)\|^2) \tag{25}$$

$$\begin{aligned}
B_2 &= \sum_{j=1}^W \sum_{i \in \mathcal{M}_j} \sum_{k=0}^{K-1} \|x_t - x_{t-j}\|^2 = K \sum_{j=1}^W m_j \|x_t - x_{t-j}\|^2 \\
&= K \sum_{j=1}^W m_j \left\| \sum_{s=0}^{j-1} (x_{t-s} - x_{t-s-1}) \right\|^2 \\
&\stackrel{(b_4)}{\leq} K \sum_{j=1}^W m_j \cdot j \sum_{s=0}^{j-1} \|x_{t-s} - x_{t-s-1}\|^2 \\
&\stackrel{(b_5)}{=} K \sum_{j=1}^W m_j \cdot j \sum_{s=0}^{j-1} \|\mathbb{E}[\Delta_{t-s-1}]\|^2 \\
&\stackrel{(b_6)}{\leq} KWM \sum_{j=1}^W \|\mathbb{E}[\Delta_{t-j}]\|^2,
\end{aligned} \tag{26}$$

where (b_4) follows $\|\sum_{i=1}^n a_i\|^2 \leq n \sum_{i=1}^n \|a_i\|^2$, (b_5) holds since there are only the items in the form of $\nabla f_i(x_{t,k}^i)$ without the form $g_{t,k}^i$, we can use $\|\mathbb{E}[\Delta_{t-s-1}]\|^2$ instead of $\|\Delta_{t-s-1}\|^2$, (b_6) follows $j \leq W$.

$$B_3 = \sum_{j=1}^W \sum_{i \in \mathcal{M}_j} \sum_{k=0}^{K-1} \|x_{t-j,k}^i - x_{t-j}\|^2 \leq \sum_{j=1}^W m_j (H_1 + H_2 \|\nabla f(x_{t-j})\|^2) \tag{27}$$

The term C is bounded as

$$\begin{aligned}
C &= \frac{\eta}{K} \left\| \frac{1}{N} \sum_{i=1}^N \sum_{k=0}^{K-1} \nabla f_i(x_{t,k}^i) - \frac{1}{N} \sum_{i=1}^N \sum_{k=0}^{K-1} \nabla f_i(x_t) \right\|^2 \\
&\stackrel{(c_1)}{\leq} \frac{\eta}{N} \sum_{i=1}^N \sum_{k=0}^{K-1} \|\nabla f_i(x_{t,k}^i) - \nabla f_i(x_t)\|^2 \\
&\stackrel{(c_2)}{\leq} \frac{\eta L^2}{N} \sum_{i=1}^N \sum_{k=0}^{K-1} \|x_{t,k}^i - x_t\|^2 \\
&\stackrel{(c_3)}{\leq} \eta L^2 (H_1 + H_2 \|\nabla f(x_t)\|^2)
\end{aligned} \tag{28}$$

where (c_1) follows $\|\sum_{i=1}^n a_i\|^2 \leq n \sum_{i=1}^n \|a_i\|^2$, (c_2) follows Assumption 1, and (c_3) follows Lemma 1.

Therefore, by putting the pieces together into Eq. (20), we obtain

$$\begin{aligned}
&\mathbb{E}[f(x_{t+1})] \\
&\leq f(x_t) - \frac{\eta K}{2} \|\nabla f(x_t)\|^2 + \frac{3M\eta L^2}{N^2} \left(M(H_1 + H_2 \|\nabla f(x_t)\|^2) + KWM \sum_{j=1}^W \|\mathbb{E}[\Delta_{t-j}]\|^2 \right. \\
&\quad \left. + \sum_{j=1}^W m_j (H_1 + H_2 \|\nabla f(x_{t-j})\|^2) \right) + \eta L^2 (H_1 + H_2 \|\nabla f(x_t)\|^2) \\
&\quad + \frac{K\eta^2 L}{2N} \sigma_L^2 - \left(\frac{1}{2\eta K} - \frac{L}{2} \right) \|\mathbb{E}[\Delta_t]\|^2.
\end{aligned} \tag{29}$$

We rewrite it as

$$\begin{aligned}
&\left(\frac{\eta K}{2} - \left(\frac{3M^2\eta L^2}{N^2} + \eta L^2 \right) H_2 \right) \|\nabla f(x_t)\|^2 - \frac{3M\eta L^2}{N^2} \sum_{j=1}^W m_j H_2 \|\nabla f(x_{t-j})\|^2 \\
&\leq f(x_t) - \mathbb{E}[f(x_{t+1})] - \left(\frac{1}{2\eta K} - \frac{L}{2} \right) \|\mathbb{E}[\Delta_t]\|^2 + \frac{3M^2 K \eta W L^2}{N^2} \sum_{j=1}^W \|\mathbb{E}[\Delta_{t-j}]\|^2 \\
&\quad + \left(\frac{6M^2\eta L^2}{N^2} + \eta L^2 \right) H_1 + \frac{K\eta^2 L}{2N} \sigma_L^2.
\end{aligned} \tag{30}$$

Here we obtain the upper bound of the t -th round. Then we rearrange the above inequalities from $t = 0$ to $T-1$ and average them, and denote the virtual items of $t = -1, -2, \dots$ (e.g., $\|\nabla f(x_{-1})\|^2$, $\|\mathbb{E}[\Delta_{-1}]\|^2$, etc.) are equal to 0. Meanwhile, suppose $\eta \leq \frac{N}{\sqrt{60(6M^2+N^2)KL}}$, there exists a constant c satisfying $0 < c < \left(\frac{1}{2} - \left(\frac{6M^2\eta L^2}{N^2} + L^2 \right) \frac{H_2}{K} \right)$. For a sufficiently large T and $K \ll T$, we have

$$\begin{aligned}
&c\eta K \frac{1}{T} \sum_{t=0}^{T-1} \|\nabla f(x_t)\|^2 \\
&\stackrel{(d_1)}{\leq} \frac{1}{T} \sum_{t=0}^{T-1} \left(\frac{\eta K}{2} - \left(\frac{6M^2\eta L^2}{N^2} + \eta L^2 \right) H_2 \right) \|\nabla f(x_t)\|^2 \\
&\leq \frac{1}{T} (f(x_0) - f(x_T)) - \frac{1}{T} \sum_{t=0}^{T-1} \left(\frac{1}{2\eta K} - \frac{L}{2} - \frac{3M^2 K \eta W^2 L^2}{N^2} \right) \|\mathbb{E}[\Delta_t]\|^2 \\
&\quad + \left(\frac{6M^2\eta L^2}{N^2} + \eta L^2 \right) H_1 + \frac{K\eta^2 L}{2N} \sigma_L^2 \\
&\stackrel{(d_2)}{\leq} \frac{1}{T} (f(x_0) - f(x_T)) + \left(\frac{6M^2\eta L^2}{N^2} + \eta L^2 \right) H_1 + \frac{K\eta^2 L}{2N} \sigma_L^2,
\end{aligned} \tag{31}$$

where (d_1) holds for $\eta \leq \frac{N}{\sqrt{60(6M^2+N^2)KL}} = \frac{1}{\sqrt{60(6r^2+1)KL}}$, (d_2) holds for $\eta \leq \frac{(\sqrt{N^2+24M^2W^2L}-N)N}{12M^2KW^2L} = \frac{\sqrt{1+24r^2W^2L}-1}{12r^2KW^2L}$ where the items containing $\|\mathbb{E}[\Delta_t]\|^2$ is eliminated.

Hence we obtain

$$\min_{t \in [T]} \|\nabla f(x_t)\|^2 \leq \frac{1}{T} \sum_{t=0}^{T-1} \|\nabla f(x_t)\|^2 \leq \frac{f(x_0) - f(x^*)}{c\eta KT} + \frac{D}{c\eta K} \quad (32)$$

where

$$\begin{aligned} D &= 5\left(\frac{6M^2}{N^2} + 1\right)(\sigma_L^2 + 6K\sigma_G^2)L^2K^2\eta^3 + \frac{K\eta^2L}{2N}\sigma_L^2 \\ &= 5(6r^2 + 1)(\sigma_L^2 + 6K\sigma_G^2)L^2K^2\eta^3 + \frac{K\eta^2L}{2N}\sigma_L^2. \end{aligned} \quad (33)$$

A.4 Visualization of Participation

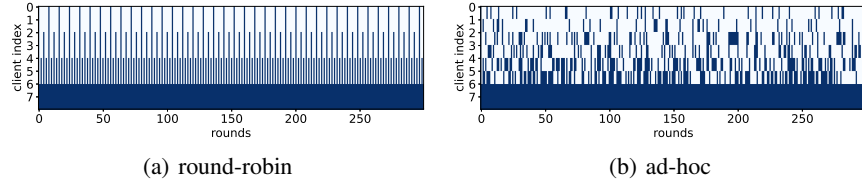


Figure 6: The visualization of participation during training process with cross-silo setting.

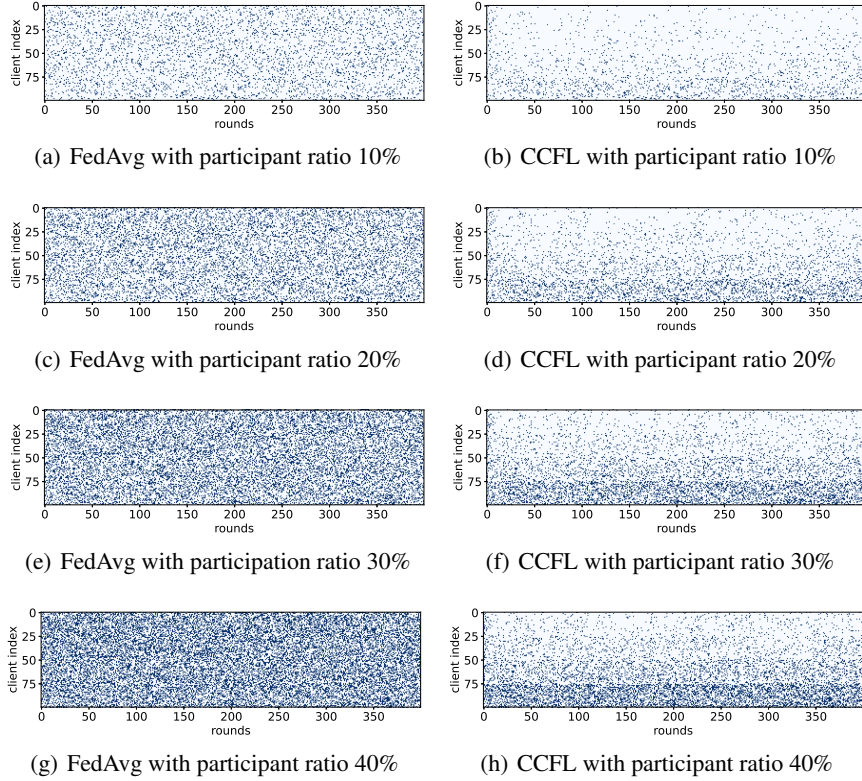


Figure 7: The visualization of participation during training process with cross-device setting.

Fig. 6 visualizes the participation of clients during training process of Table 1 with round-robin and ad-hoc schedules, respectively. Client x participates (does not participate) in round y is shown by

the dark (light) color at (x, y) . From the figure, we can intuitively see the difference of participation rounds across clients, and CCFL spends much fewer computational resources than vanillar federated learning (in this situation all the points in the figure are dark).

Fig. 7 visualizes the participation of clients during training process of Table 2, Table 3 and Table 4. Due to cross-device setting, the participation of one client in CCFL is determined by both sever selection and client decision (on the contrary, the participation of one client in FedAvg is only determined by sever selection). Fig. 7(a) and Fig. 7(b) visualize the actual participation in training where the server selects 10% clients in each round. It is obvious that CCFL needs much fewer participation than FedAvg. The similar situations are shown from Fig. 7(c) to Fig. 7(h).

A.5 Extra Experiments under Cross-device Settings

Table 3: Performance (top-1 validation accuracy) comparison on FMNIST with different data heterogeneity, where $N = 100$ and $\beta = 4$, and the classes of training data are highly skewed across clients with different computational resources.

	10%	20%	30%	40%
FedAvg	67.78 \pm 7.35	70.51 \pm 4.68	75.25 \pm 2.51	76.86 \pm 2.26
Strategy 1	55.30 \pm 9.11	58.59 \pm 8.56	58.60 \pm 6.54	60.17 \pm 5.68
Strategy 2	52.40 \pm 8.29	60.24 \pm 6.69	69.37 \pm 3.37	71.75 \pm 3.14
CCFL	58.47\pm9.86	66.11\pm6.32	70.99\pm 4.19	73.89\pm3.62

Table 4: Performance (top-1 validation accuracy) comparison on FMNIST with different data heterogeneity, where $N = 100$ and $\beta = 4$, the classes of training data are moderately skewed across clients with different computational resources.

	10%	20%	30%	40%
FedAvg	74.52 \pm 3.63	80.14 \pm 2.07	81.03 \pm 1.86	81.62 \pm 1.11
Strategy 1	65.64 \pm 5.77	74.92 \pm 4.40	77.53 \pm 2.89	78.29 \pm 2.37
Strategy 2	59.16 \pm 5.88	71.26 \pm 4.03	75.17 \pm 3.12	76.97 \pm 1.67
CCFL	70.14\pm4.05	78.40\pm2.17	79.30\pm 2.90	80.36\pm1.61

In Table 2 each client is randomly assigned two types of data. Each class of data is spread evenly among 10 clients. We assign p_i at random (i.e., we randomly assign the computational resources). Each type of data is present on both the clients with adequate resources and the clients with insufficient resources. Therefore, the data distribution is not skewed during training. In practice, missing some clients may skew the real-time training data. Table 3 and Table 4 study the impact, respectively. In Table 3 we assign two classes of data two 20 clients randomly, and assign the same p_i to the clients with the same class of data. As a consequence, each class of data is either on the client with adequate resources or the clients with insufficient resources. The data distribution is significantly skewed during training. Compared with Table 2, in this situation the performance of CCFL deteriorates more. But compared with the other two strategies, this method is much more robust. For example, when participant ratio is 20%, compared to FedAvg, CCFL reduces the performance by only 4%, while the performance is deteriorated by more than 10% by another two strategies. Furthermore, in Table 2 Strategy 1 is better than Strategy 2 in most cases, but the result is reversed in Table 2. On the contrary, CCFL is consistent under the varying of settings. Table 4 also verifies the advantages of CCFL, which is a compromise between Table 2 and Table 3, with only 10% of clients using the setting of Table 3 (these clients have adequate resources) and the rest following the setting of Table 2. Correspondingly, the data distribution is moderately skewed during training.

A.6 Influence of r and W

To compare with baselines, we also investigate the model performance of Strategy 1 and Strategy 2 with different r and W . Fig. 8 corresponds to Fig. 4(a), and Fig. 9 corresponds to Fig. 4(b). We can find CCFL performs stable under most r and W , while Strategy 1 and Strategy 2 degrade severely with moderately large r or W .

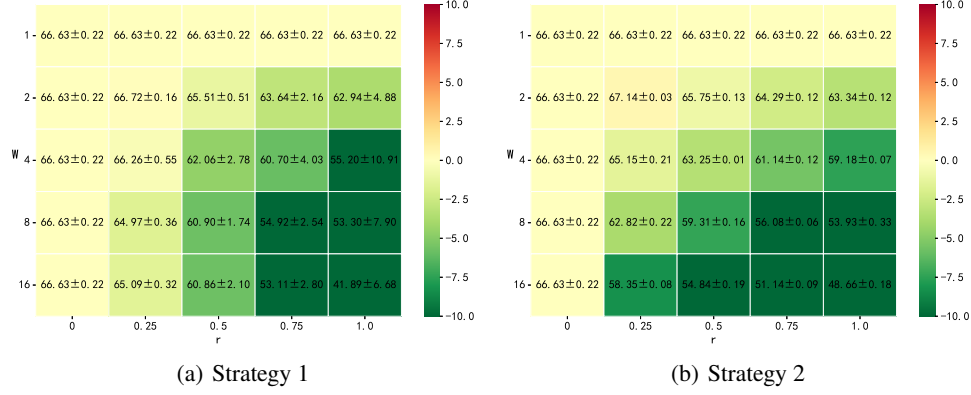


Figure 8: The performance changes with varying of r and W under cross-silo scenarios (CIFAR-10).

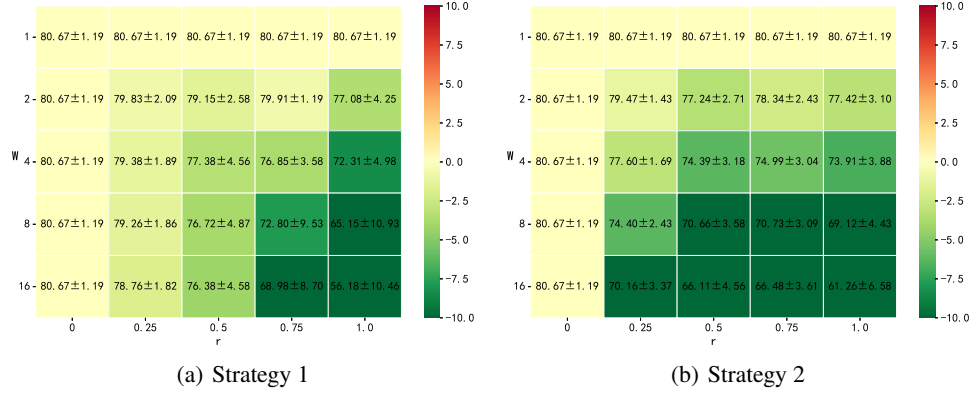


Figure 9: The performance changes with varying of r and W under cross-device scenarios (FMNIST).

A.7 Extra Experiments for CCFL($r = 1$)

For CCFL($r = 1$) in Fig. 5 each client skips or performs local training in ad-hoc schedule individually. In each round, there will always be clients undertaking local training to keep true information in aggregation. If we synchronize the rhythm of all clients that skipping or performing training in all rounds, CCFL becomes similar as FedOpt [35] (we denote CCFL in this situation as CCFL(synchronization)). For example, if all clients estimate local models in sequential $W - 1$ rounds after execute local training

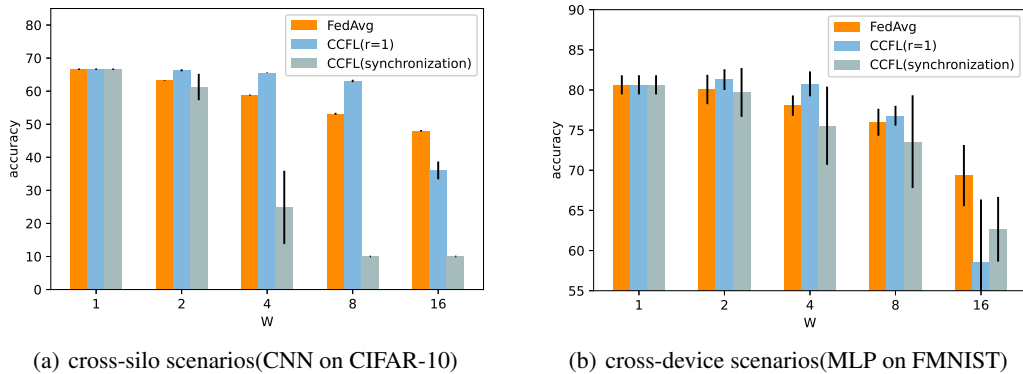


Figure 10: Efficiency comparison between CCFL($r = 1$) with FedAvg and FedOpt(W).

in one round (denote as round t), the aggregated model at round $t + W - 1$ are $x_t + (W - 1)\Delta_t$, where $(W - 1)$ can be viewed as the global learning rate in FedOpt. In Fig. 10 we add the comparison between CCFL(synchronization) and CCFL($r = 1$) based on Fig. 5. It shows CCFL(synchronization) performs much worse than CCFL($r = 1$), even worse than FedAvg. Therefore, ad-hoc schedule plays a vital role to keep CCFL's performance.